

11-2018

Investigation on the RONS and Bactericidal Effects Induced by He + O₂ Cold Plasma Jets: In Open Air and in an Airtight Chamber

Han Xu

Dingxin Liu


Weitao Wang

Zhijie Liu

Li Guo

See next page for additional authors

Follow this and additional works at: https://digitalcommons.odu.edu/bioelectrics_pubs

 Part of the [Biomedical Engineering and Bioengineering Commons](#), [Electrical and Computer Engineering Commons](#), and the [Plasma and Beam Physics Commons](#)

Repository Citation

Xu, Han; Liu, Dingxin; Wang, Weitao; Liu, Zhijie; Guo, Li; Rong, Mingzhe; and Kong, Michael G., "Investigation on the RONS and Bactericidal Effects Induced by He + O₂ Cold Plasma Jets: In Open Air and in an Airtight Chamber" (2018). *Bioelectrics Publications*. 227.

https://digitalcommons.odu.edu/bioelectrics_pubs/227

Original Publication Citation

Xu, H., Liu, D., Wang, W., Liu, Z., Guo, L., Rong, M., & Kong, M. G. (2018). Investigation on the rons and bactericidal effects induced by He + O₂ cold plasma jets: In open air and in an airtight chamber. *Physics of Plasmas*, 25(11), 113506. doi:10.1063/1.5055802

Authors

Han Xu, Dingxin Liu, Weitao Wang, Zhijie Liu, Li Guo, Mingzhe Rong, and Michael G. Kong

Investigation on the RONS and bactericidal effects induced by He + O₂ cold plasma jets: In open air and in an airtight chamber

Han Xu, Dingxin Liu, Weitao Wang, Zhijie Liu, Li Guo, Mingzhe Rong, and Michael G. Kong

Citation: [Physics of Plasmas](#) **25**, 113506 (2018); doi: 10.1063/1.5055802

View online: <https://doi.org/10.1063/1.5055802>

View Table of Contents: <http://aip.scitation.org/toc/php/25/11>

Published by the [American Institute of Physics](#)

Articles you may be interested in

[An atmospheric pressure plasma jet operated by injecting natural air](#)

[Applied Physics Letters](#) **113**, 194101 (2018); 10.1063/1.5055592

[Study on spatiotemporal dynamic and spectral diagnosis of snowflake pattern in dielectric barrier discharge](#)

[Physics of Plasmas](#) **25**, 113507 (2018); 10.1063/1.5042306

[Comparison between the water activation effects by pulsed and sinusoidal helium plasma jets](#)

[Physics of Plasmas](#) **25**, 013520 (2018); 10.1063/1.5016510

[Production and correlation of reactive oxygen and nitrogen species in gas- and liquid-phase generated by helium plasma jets under different pulse widths](#)

[Physics of Plasmas](#) **25**, 013528 (2018); 10.1063/1.4999520

[Guided ionization waves: The physics of repeatability](#)

[Applied Physics Reviews](#) **5**, 031102 (2018); 10.1063/1.5031445

[Average electron temperature estimation of streamer discharge in ambient air](#)

[Review of Scientific Instruments](#) **89**, 113502 (2018); 10.1063/1.5027836

Investigation on the RONS and bactericidal effects induced by He + O₂ cold plasma jets: In open air and in an airtight chamber

Han Xu,¹ Dingxin Liu,^{1,a)} Weitao Wang,¹ Zhijie Liu,^{1,a)} Li Guo,¹ Mingzhe Rong,¹ and Michael G. Kong^{1,2,3}

¹State Key Laboratory of Electrical Insulation and Power Equipment, Centre for Plasma Biomedicine, Xi'an Jiaotong University, Xi'an 710049, People's Republic of China

²Frank Reidy Center for Bioelectrics, Old Dominion University, Norfolk, Virginia 23508, USA

³Department of Electrical and Computer Engineering, Old Dominion University, Norfolk, Virginia 23529, USA

(Received 11 September 2018; accepted 19 October 2018; published online 8 November 2018)

He + O₂ plasma jets in open air and in an airtight chamber are comparatively studied, with respect to their production of gaseous/aqueous reactive species and their antibacterial effects. Under the same discharge power, the plasma jet in open air has higher densities of gaseous reactive species and a higher concentration of aqueous H₂O₂ but lower concentrations of aqueous OH and O₂⁻. In addition, the increase in the O₂ ratio in He in both plasma jets causes a linear decrease in the population of gaseous reactive species, except for O(3p⁵P) when a small amount of O₂ is added to the working gas. The concentrations of aqueous reactive species for OH and H₂O₂ also drop monotonically with the increase in additive O₂, while the aqueous O₂⁻ first increases and then decreases. Moreover, it is interesting that the bactericidal inactivation in the airtight chamber condition is much greater than that in the open air condition regardless of the presence or absence of additive O₂ in the He plasma jet. The concentration trends of O₂⁻ for both the plasma jets are similar to their antibacterial effects, and little antibacterial effect is achieved when a scavenger of O₂⁻ is used, indicating that O₂⁻ should be a main antibacterial agent. Moreover, it should not be O₂⁻ alone to achieve the antibacterial effect, and some reactive nitrogen species such as ONOO⁻ and O₂NOO⁻ might also play an important role. *Published by AIP Publishing.*

<https://doi.org/10.1063/1.5055802>

I. INTRODUCTION

In recent years, cold atmospheric pressure plasmas have attracted considerable attention for use in various medical and biological applications such as cancer therapy,^{1,2} enhanced wound healing,^{3–5} inactivation of pathogenic amyloids,^{6,7} disinfection of the human body or teeth,^{8–10} sterilization,^{11–17} and so on. Among these applications, aqueous reactive oxygen species (ROS) and reactive nitrogen species (RNS) produced by gas plasmas are considered to be the key constituents.^{18–21} From previous simulation and experimental works, it is widely accepted that generation and doses of aqueous reactive species are related to the mass transfer of upstream plasmas and chemical reaction in the liquid phase.^{22–24} In terms of application requirements, it is necessary to obtain a quantitative correlation between specific characteristics of upstream plasmas, composition and concentration of aqueous reactive species, and the biological effects. Simultaneously, to determine the components and doses of the key reactive species, finding out the links between them also helps us find the optimal control strategy for different applications. However, the relationship between the three is very complex and is a key challenge for plasma science.

As a main way for discharge, atmospheric pressure plasma jets (APPJs) have the indubitable advantage that they

are able to transport the plasma with various reactive species to a separate region for treatment applications. In addition, many research groups have studied that the biological effect of the plasma jet can be significantly improved when the additive O₂ is added into the working gas, for the concentrations of several ROS which are considered to play an important role are increased a lot.^{25–27} But research studies also show that the concentration of ROS and the biological effect are not continuously enhanced with the increase in additive O₂.^{26–29} For example, Joh *et al.*³⁰ have demonstrated that the best plasma treatment effect on the apoptosis of human bladder cancer cells can be achieved in He + 2% O₂ for an atmospheric pressure pulsed plasma jet, and the same fraction of additive O₂ also applies for the bacterial inactivation studied by Bai *et al.*²⁴ In the above studies, there would inevitably be air mixing into plasma as the plasma jet in open air. However, certain study reports that the afterglow gas of He + O₂ plasma (without the air mixing) can also lead to high bactericidal activity, and this afterglow gas can be used for sterilization.³¹ To our knowledge, the comparison of the plasma jet in open air and in an airtight chamber has rarely been reported before. Therefore, how much the concentrations of aqueous reactive species can be affected by air mixing in the interaction of He + O₂ plasma and aqueous solution? What is the impact on biological effects? These issues need to be researched thoroughly.

In this paper, a quartz chamber is added to the nozzle of the quartz tube to exclude the air inclusion, which enables a

^{a)}Electronic mail: liudingxin@mail.xjtu.edu.cn and liuzhijie2010@163.com

plasma jet to discharge in the open air condition and in the airtight chamber condition. Thus, an experimental study is carried out to directly compare the electrical characteristics, the optical emission spectra, and the bacterial inactivation efficiency with different O₂ contents for the two plasma jets. Using chemical fluorescent probes and electron spin resonance (ESR) spectrometry, concentrations of several ROS induced by two plasma jets have been measured quantitatively to clearly show their differences. Finally, several groups of bactericidal control experiments are done to explain the underlying mechanism of the sterilization.

II. EXPERIMENTAL SETUP AND METHODS

Our experiments are conducted with two plasma-water systems as shown in Fig. 1(a). The only difference between these two systems is whether an airtight chamber is used. Without the airtight chamber, the plasma plume is generated in open air, and hence, a large amount of air (N₂, O₂ and H₂O) would inevitably be mixed into the working gas. Otherwise, the air inclusion could be neglected, and only the evaporation of the treated water could change the working gas composition to some extent. For either the plasma jet source, the high voltage electrode is made of a stainless steel rod with a diameter of 1 mm, which is placed on the axis of a quartz tube with an outer diameter of 6 mm and an inner diameter of 4 mm. The needle tip of the high voltage electrode has a distance of 10 mm from the nozzle of the quartz tube, and there is a 10 mm long grounded ring electrode positioned near the end of the glass tube. A glass dish with 2 ml deionized water (DW) or bacterial suspension is located

5 mm away from the jet nozzle. He and O₂ flow through the quartz tube, and the O₂-to-He ratio (from 0.5% to 4%) is controlled by mass flow controllers (Brooks 5850E) with a total rate of 2 SLM. The needle-ring electrode structure can stably generate the plasma jet in open air and in the airtight chamber.

Sinusoidal power supply with a frequency of 20 kHz is used to generate plasma. The waveforms of discharge voltage and current are recorded by an oscilloscope (Tektronix, DPO3000) with a high-voltage probe (Tektronix, P6015A) and a current probe (Tektronix, P6021). The discharge power is obtained by integration of the voltage and current waveforms. In order to directly compare the impact of the ambient air and different proportions of additive O₂ for the He plasma jet, the two plasma jets are controlled with the same discharge power of ~ 1 W, which is obtained by integration of the measured voltage of the high voltage electrode and current of the grounded electrode.

The discharge images taken by a digital camera (Nikon D7000) for the plasma jet in open air and in the airtight chamber as a function of the O₂ content are shown in Figs. 1(b) and 1(c), respectively. It can be seen that the brightness of the plasma plumes is obviously weaker with the increasing O₂ fraction for the two plasma jets. The plasma plume length also decreases with increase in the O₂ concentrations, but the plasma plume of the plasma jet in open air and in the airtight chamber can touch the water surface in the discharge power of $P = 1$ W. The plasma plume effectively contacting the water surface is a significant experimental condition, which can have a great impact on the concentrations of several aqueous reactive species such as OH.^{32,33}

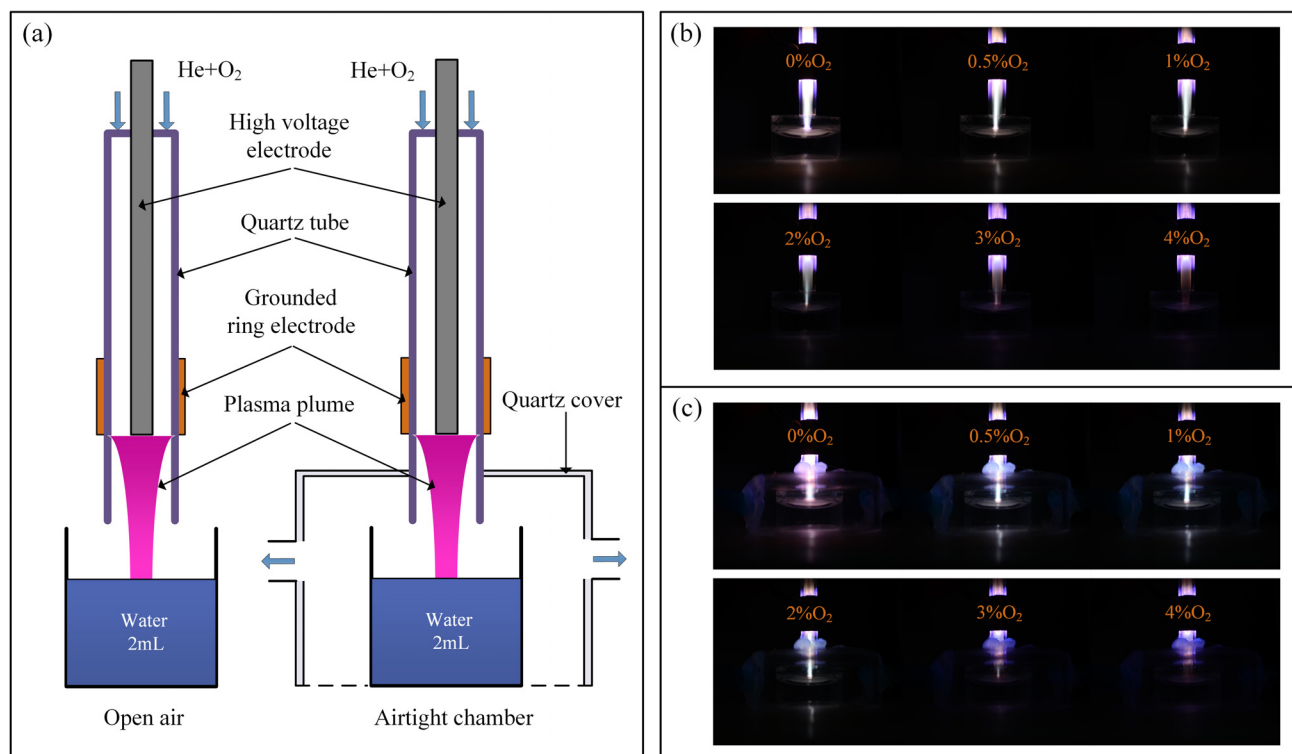


FIG. 1. Schematic diagram of the experimental system (a) and the discharge images [(b) and (c)] with different O₂ contents for the plasma jets in open air and in the airtight chamber.

Excited gaseous reactive species generated by plasma jets in the two conditions are measured using an optical emission spectrometer (Ocean Optics, USB2000) at the nozzle of the quartz tube, and the detected spectral range is between 200 and 800 nm. All optical diagnostics are done with the water sample in place.

The pH of the treated DW is measured with a pH meter (METTLER TOLEDO FE28). Aqueous reactive species in DW are measured quantitatively with up to 3 min plasma treatment. For long-lived species NO_2^- , NO_3^- , and H_2O_2 , their absolute concentrations are measured by chemical fluorescent assays including Griess reagent (for $\text{NO}_2^-/\text{NO}_3^-$) and Amplex[®] Red reagent (for H_2O_2). All chemicals and measurements on these three long-lived species are done following the protocols provided by assay manufacturers. However, no detectable signal is detected, indicating that the concentration of $\text{NO}_2^-/\text{NO}_3^-$ is lower than the detection limit of $\sim 1 \mu\text{M}$. Two representative aqueous short-live species including OH and O_2^- are measured by ESR (Bruker BioSpin GmbH, EMX) spectroscopy using their correspondent spin traps, which can capture them into stable spin trap adducts. DMPO (5,5-dimethyl-1-pyrrolineN-oxide, Dojindo, 50 mM) is used to capture OH to generate DMPO-OH and TEMPONE-H (1-Hydroxy-2,2,6,6-tetramethyl-4-oxo-piperidine, Enzo, 1 mM) is used to react with O_2^- to produce TEMPONE.^{34,35} It should be noted that TEMPONE-H can also capture peroxyxynitrite (ONOOH and ONOO^-) and NO_2 , and the product is also TEMPONE.³⁶ So, the concentration of TEMPONE represents the total concentration of O_2^- , peroxyxynitrite ($\text{ONOO}^-/\text{ONOOH}$), and NO_2 . Thus, a scavenger of O_2^- , superoxide dismutase from bovine erythrocytes (SOD, Sigma, USA, $100 \mu\text{g}\cdot\text{ml}^{-1}$), is added into the water together with the TEMPONE-H to obtain the final aqueous concentration of O_2^- .^{18,37} In order to capture all these radicals, spin traps are added into DW before plasma treatment. In ESR experiments, 3360 G of center magnetic field and 20 mW microwave power are used to make these radicals resonating. Intensity results from ESR are calibrated by the stable radical TEMPO into concentrations.

In the sterilization experiment, *Staphylococcus aureus* (*S. aureus*) is chosen for plasma treatment. As a test microorganism, *S. aureus* is cultured in 4 ml TSB liquid medium first for 12 h. Part of the culture ($300 \mu\text{l}$) is transferred into 30 ml TSB liquid medium to amplify culture for 3 h and then pelleted by centrifugation at 4000 rpm for 3 min, after which it is resuspended in physiological saline solution to $\text{OD}_{600} = 0.75$, approximately 3×10^8 colony-forming units/ml ($\text{cfu}\cdot\text{ml}^{-1}$). Finally, the prepared bacterial suspension is diluted to different final concentrations for treatments in open air and in the airtight chamber, respectively.

In the control group of bactericidal experiments, SOD ($100 \mu\text{g}\cdot\text{ml}^{-1}$) which has a scavenging effect on O_2^- is included in the bactericidal assay as a control group for DW. In addition, Bovine Serum Albumin, BSA (WAKO Pure Chemicals, $100 \mu\text{g}\cdot\text{ml}^{-1}$), is used for a control of SOD. BSA is a protein without enzymatic activity to quench O_2^- in biochemistry, which can exclude the effect of SOD's protein properties on the sterilization effect.^{38,39}

III. RESULTS AND DISCUSSION

A. Gaseous reactive species

In Figs. 2(a) and 2(b), the discharge current and voltage waveforms with He + 3% O_2 for plasma jets in open air and in the airtight chamber are recorded. In our experiment, all the electrical characteristics with the increase in the O_2 fraction are measured. Herein, only the He + 3% O_2 is displayed. With the same power dissipated into the jet device, voltages and currents measured in two discharge conditions illustrate a very similar form. However, the discharge voltage of the plasma jet in open air is less than that in the airtight chamber, and for the current, it is just opposite. In addition, the change trends of the peak-to-peak discharge voltage as a function of the O_2 content for the two discharge conditions are shown in Fig. 2(c). The results show that the discharge voltages first decrease and then increase with the increase in O_2 contents under the same discharge power for

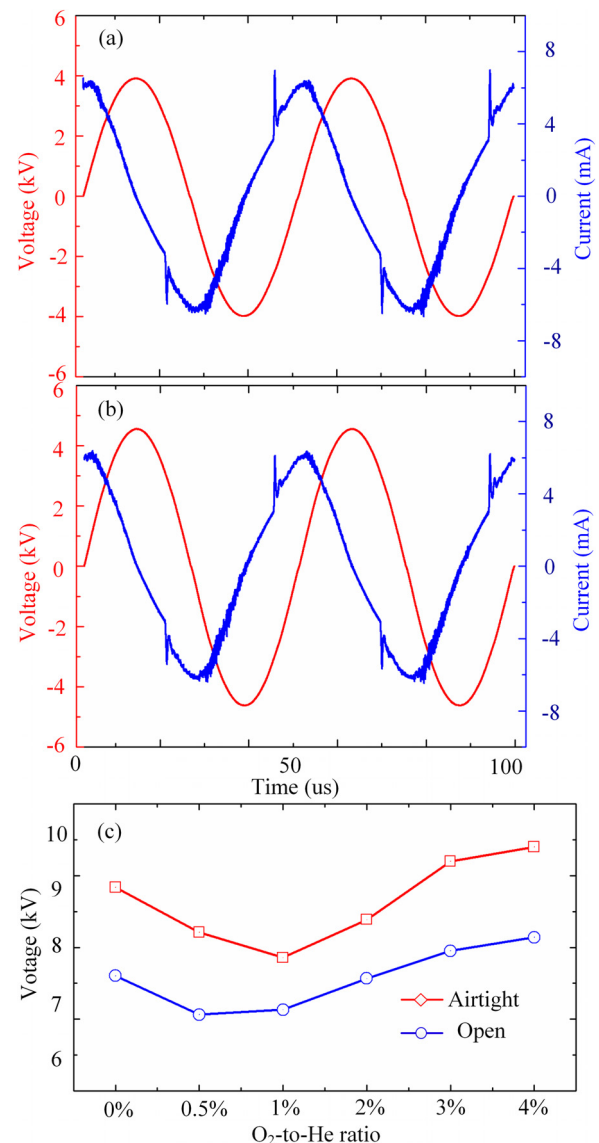
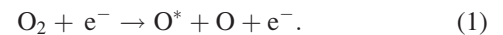


FIG. 2. I-V characteristics of the plasma jets with the working gas of He + 3% O_2 in open air (a) and in the airtight chamber (b), as well as the peak-to-peak voltage of the discharge as a function of the O_2 content for the two discharge conditions (c).

the two plasma jets. For the plasma jet in the airtight chamber, the peak-to-peak voltage decreases from 8.8 kV to 7.9 kV when the O₂ percentage varies from 0% to 1%, and then the voltage rises to 9.4 kV when 4% O₂ is added. However, with respect to the plasma jet in open air, the lowest voltage is 7.1 kV at 0.5% O₂, and the voltage reaches up to 8.1 kV at 4% O₂. The addition of a small amount of O₂ can promote penning ionization that causes the reduction of voltage when the power is kept constant.⁴⁰ However, the fast moving electrons can be transformed into slow moving anions with the electronegative characteristics of O₂.^{26,29} Thus, the higher voltage is needed to sustain the discharge when more additive O₂ is added into the working gas. In addition, the discharge voltage of the plasma jet in open air is lower than that in the airtight chamber, which may be attributed to the Penning ionization of N₂ from air, because N₂ is not an electronegative gas and electrons would not be adsorbed.²⁹

The optical emission spectra of the plasma plume with the increase in O₂ percentage are measured. Figures 3(a) and 3(b) show the emission spectra of the plasma jet in He + 1% O₂ and He + 3% O₂ for the open air condition and the airtight chamber condition, respectively. The reason why these two ratios are selected is that the best bactericidal effect can be achieved for the two plasma jets, which is shown in the sterilization experiment below. Besides, the emission

intensities of the reactive species including OH(A), N₂(C), He(3s³S), and O(3p⁵P) which have strong emission lines at 309, 337, 706, and 777 nm are shown in Figs. 3(c) and 3(d). The results show that the emission intensities of OH(A), N₂(C), and He(3s³S) decrease with the increase in additive O₂ for the two plasma jets, and the emission intensities are almost undetectable when 3% or more O₂ is added to the He gas. The weaker discharge and reduced reactive species after the addition of O₂ can explain the phenomenon. However, compared with the other three species, the relative emission intensity of O(3p⁵P) in the whole optical emission spectrum increases when a small amount of O₂ is added to the working gas. It can be seen that the emission intensity of O(3p⁵P) is higher than that of other reactive species for the two plasma jets, when the proportion of additive O₂ is less than 2% since electron impact dissociative excitation of O₂ is the main channel to populate the emitting oxygen level from 3p⁵P to 3s⁵S at 777 nm [Eq. (1)],^{24,41} which means that more electrons are consumed to produce O radicals with the additive O₂ in the same discharge power



In addition, N₂(C) or other nitrogen metastable species are not detected in the airtight chamber condition, which also proves that the air in the quartz chamber is indeed ruled out and the tightness is good.

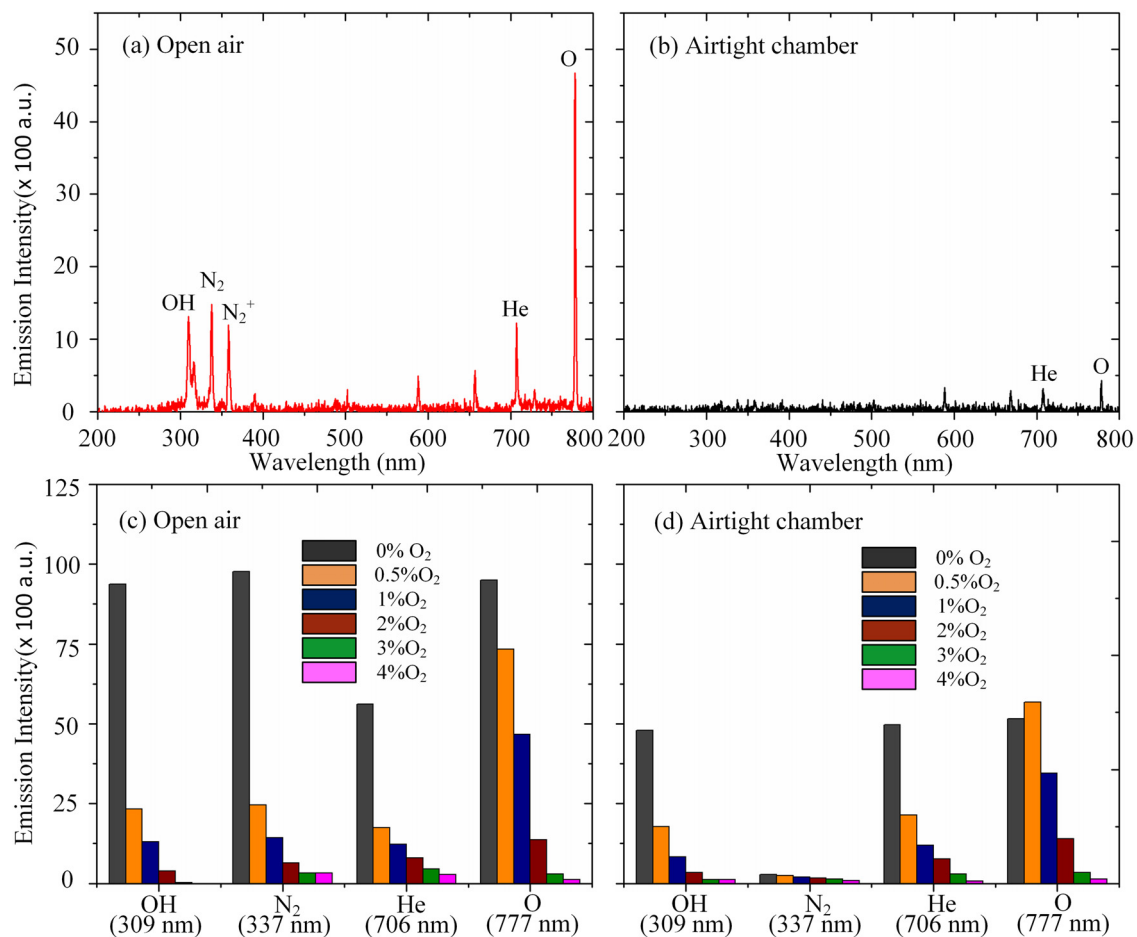


FIG. 3. The emission spectra for the plasma jets in open air with He + 1% O₂ (a) and in the airtight chamber with He + 3% O₂ (b). Comparison of the changes in the emission intensities of OH, N₂, He, and O radicals as a function of the O₂ content in open air (c) and in the airtight chamber (d).

B. Bactericidal effects and aqueous reactive species

In the bactericidal experiment in this paper, the bacterial suspensions are incubated for 5 min after 3 min of the plasma treatment and then diluted with PBS immediately. Tenfold serial dilutions of microorganism suspension are plated on TSB agar and incubated for 24 h, after which colonies are counted to determine the number of viable microorganisms ($\text{cfu}\cdot\text{ml}^{-1}$). For the control experiments, the bacterial samples are treated using the same plasma sources but without the applied voltage, i.e., the gas flow rate is the same but the plasma is off. The sterilization phenomenon images are taken by the digital camera (Nikon D7000) with an exposure time of 1 s.

Figure 4 shows the bacterial inactivation results for the two plasma jets with respect to the different O_2 concentrations in the feeding gas. According to the results of the preliminary experiment (not shown in the paper), the initial concentrations of the treated bacterial suspensions are selected as $\sim 10^6$ CFU/ml and $\sim 10^7$ CFU/ml for the plasma jet in open air and in the airtight chamber, respectively. There is no bactericidal effect for the plasma jet in open air with or without the additive O_2 , when the bacterial culture is

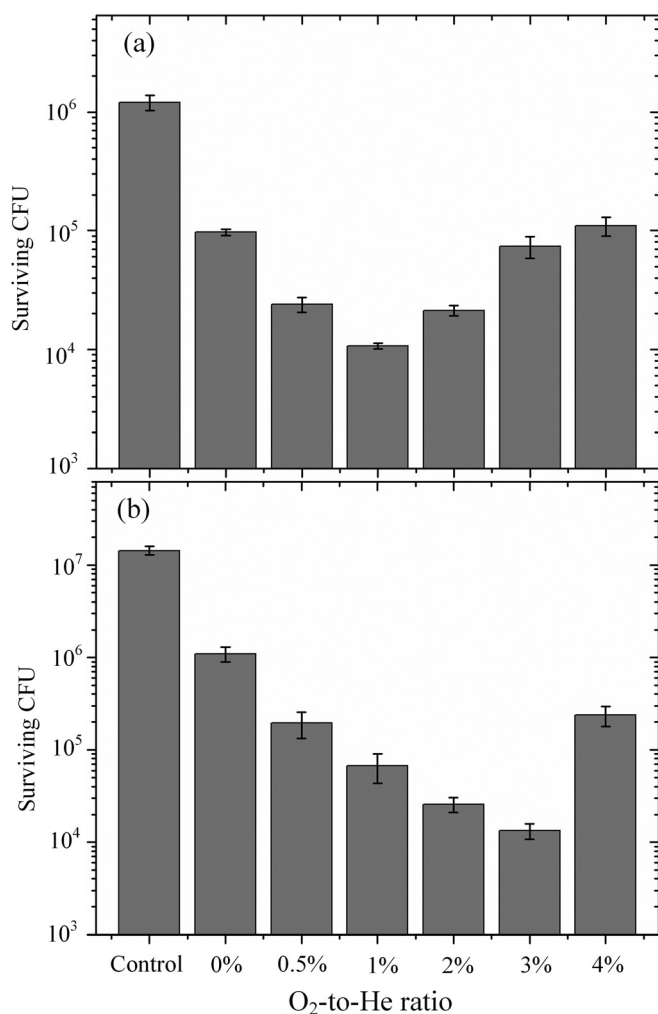


FIG. 4. Number of surviving cells in the solution after 3 min plasma treatment as a function of the O_2 content for the plasma jets in the open air condition (a) and the airtight chamber condition (b), respectively.

$\sim 10^7$ CFU/ml. So, the most important result is that the bactericidal effect of the plasma jet in the airtight chamber is much greater than that in open air, even for the plasma jet under pure He. Besides, the results also show that the concentrations of *S. aureus* after treated by the two plasma jets first decrease and then increase as a function of the O_2 fraction. In particular, the residual bacterial concentration minimizes at the O_2 fraction of 1% for the open air condition, but for the airtight chamber condition, it delays to 3%. When the initial concentration of the bacterial culture is $\sim 10^6$ CFU/ml, the surviving cell numbers decrease by more than one order of magnitude after 3 min treatment by the plasma jet in open air with pure He. The bacterial reduction increases to ~ 2 logs with the addition of 1% O_2 to the He gas, which proves that the bactericidal effect of the plasma jet can be improved when the right amount of O_2 is added into the working gas. For the plasma jet in the airtight chamber, the cell concentration is shown to have decreased nearly 10^3 times in He + 3% O_2 under the same discharge power, and even the concentration of bacterial culture is increased by 10 times.

There are many reports that aqueous ROS contribute to bacterial inactivation for the plasma treatment. Zhang et al.⁴² and Traylor et al.⁴³ have proposed that H_2O_2 plays an important role in bacterial inactivation. In addition, certain studies demonstrate that the aqueous OH is the most important reactive species for the sterilization.²⁵ Moreover, several reports suggest that O_2^- and its direct conjugate, hydroperoxy radicals (HOO), play an important role in the initiation of the oxidation of the fatty acid in the cell membrane, thus leading to the inactivation of microorganism.^{18,37,44,45} In order to figure out exactly which reactive species have key functions in our plasma-based bacterial inactivation, it is essential to measure the concentrations of these RONS in the liquid phase.

The pH value and the concentrations of several aqueous ROS induced by the two plasma jets are shown in Fig. 5, as a function of O_2 concentration from 0% to 4%. As shown in Fig. 5(a), untreated DW has an initial pH of ~ 6.8 . After 3 min treatment of plasma jets in open air or in the airtight chamber, the pH value has dropped from ~ 6.8 to ~ 3.8 . Interestingly, the pH value is almost unchanged with the increase in O_2 contents for the two plasma jets, indicating that additive O_2 has little influence on the pH value of the solution in the discharge. It has reported that the pH value plays a crucial role in liquid sterilization. A high bactericidal effect using plasma jets has been achieved in liquids via the reduced pH method where the solution is sufficiently acidic.^{44,46} Besides, there are reports suggesting that there is a critical pH value of ~ 4.7 for bactericidal effects to occur. Bacteria in aqueous solution can be efficiently inactivated below the critical pH value, whereas they are hardly affected by plasma treatment above this pH value.^{44,47} Thus, the pH value of bactericidal treatment is satisfied under our experimental conditions.

As illustrated in Figs. 5(b) and 5(c), the concentrations of the aqueous H_2O_2 and spin adduct DMPO-OH decrease in the same discharge power as a function of the additive O_2 for the two plasma jets. However, there is also a difference between the trends of the concentration of the two species.

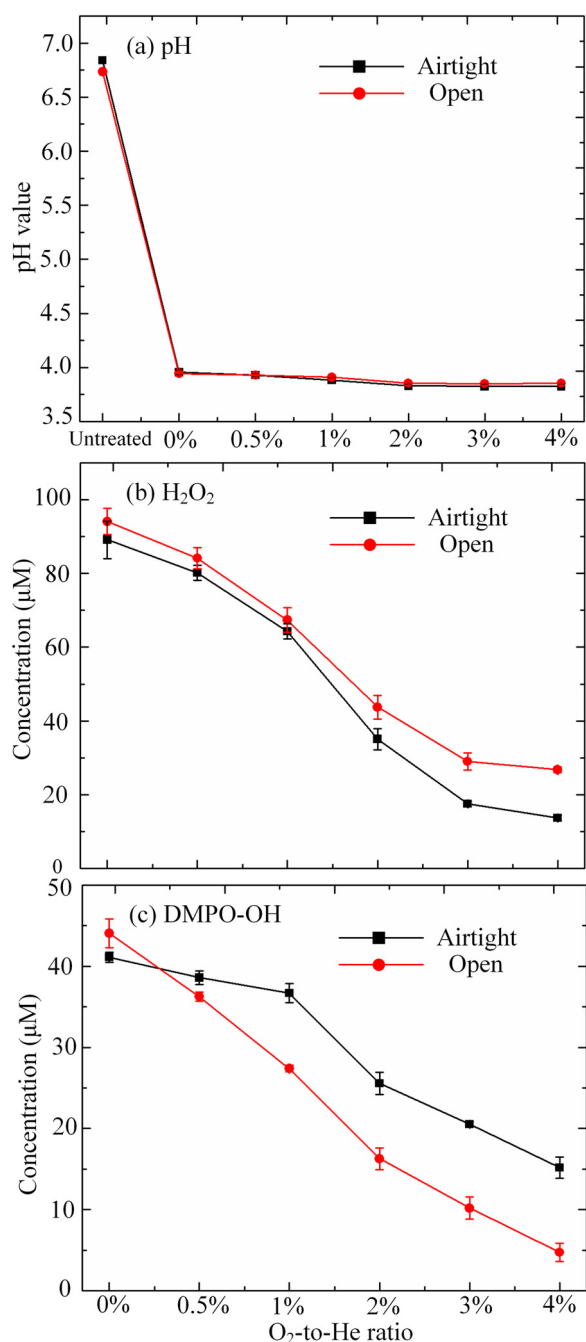
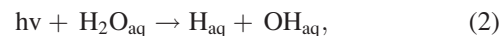


FIG. 5. The pH value (a) and concentrations of H_2O_2 (b) and DMPO-OH (c) in the solution after 3 min plasma treatment as a function of the O_2 content for the two plasma jets in the open air and in the airtight chamber.

The concentration of H_2O_2 induced by the plasma jet in open air is always higher than that in the airtight chamber with the increasing additive O_2 , but for the concentration of spin adduct DMPO-OH, it is opposite. The concentrations of H_2O_2 in the open air condition and in the airtight chamber condition with pure helium are $94.1 \mu\text{M}$ and $89.1 \mu\text{M}$, respectively; then, the concentrations drop to $26.8 \mu\text{M}$ and $13.7 \mu\text{M}$, respectively, with the addition of 4% O_2 to the He gas. The concentration of DMPO-OH decreases from $44.1 \mu\text{M}$ to $4.7 \mu\text{M}$ when the working gas changes from He to He + 4% O_2 for the plasma jet in open air. In the airtight chamber condition, the concentration decreases from $41.1 \mu\text{M}$ to $15.2 \mu\text{M}$. According to the recent reports by our

group and others,^{32,48} the main pathway for the production of aqueous H_2O_2 is the solvation of gaseous H_2O_2 , which is largely generated inside the plasma tube. In plasma systems involving humid gas or direct contact with aqueous solutions, the aqueous OH is partly derived from the solvation of gaseous species, and some of it is generated directly at the gas-liquid interface^{33,49}



In Eqs. (2) and (3), aqueous OH is formed through photodissociation of water and charge exchange of incident positive ions on the gas-liquid surface. So, the concentration of DMPO-OH induced by the plasma jet in the airtight chamber is higher than that in open air, which may be attributed to the fact that the production of aqueous OH is hindered by the air mixing at the gas-liquid interface. However, the H^+ element is increased thanks to the mixing of air during the plasma generation process, which is conducive to the production of H_2O_2 for the open air condition. Besides, the addition of O_2 into the feeding gas tends to diminish the production of radicals due to the electron attachment to O_2 inside the nozzle.^{26,29} This is the reason that the concentrations of the two reactive species decrease and the discharge become weakened with the additive O_2 , which also corresponds to the change in the intensities of the optical emission spectrum. In addition, the results also show that the aqueous H_2O_2 and OH are not the main bactericidal substances in our experiments, for the trends of the concentrations with the additive O_2 do not agree with the bactericidal effect.

Figure 6 shows the concentrations of the spin adduct TEMPONE and aqueous O_2^- as a function of the O_2 content for the two plasma jets. It is worth noting that the concentrations of them with the addition of 5% O_2 to the He gas are measured in order to better study its variation trend. It can be seen that the concentration of the spin adduct TEMPONE increases with the increase in the O_2 fraction, which is exactly opposite to the variation trend of the concentrations of H_2O_2 and DMPO-OH in Fig. 5. Besides, the concentration of TEMPONE induced by the plasma jet in the airtight chamber is higher than that in open air as the O_2 is added to the He gas. The concentration of TEMPONE increases from $7.2 \mu\text{M}$ to $37.1 \mu\text{M}$ when the working gas changes from He to He + 4% O_2 for the airtight chamber condition, and for the open air condition, the concentration increases from $8.8 \mu\text{M}$ to $33.2 \mu\text{M}$. As mentioned above, SOD ($100 \mu\text{g}\cdot\text{ml}^{-1}$) is added into the water together with the TEMPONE-H to obtain the final aqueous concentration of O_2^- , which is shown in Fig. 6(b). It should be noted that the used amount of SOD is large enough, i.e., the concentration of TEMPONE does not decrease anymore with the increased amount of SOD. Moreover, the difference value between the TEMPONE concentrations with and without the use of SOD represents the concentration of trapped O_2^- . It can be seen that the concentration of O_2^- in the airtight chamber condition is always higher than that in the open air condition, no matter with or without the additive O_2 . For the plasma jet in

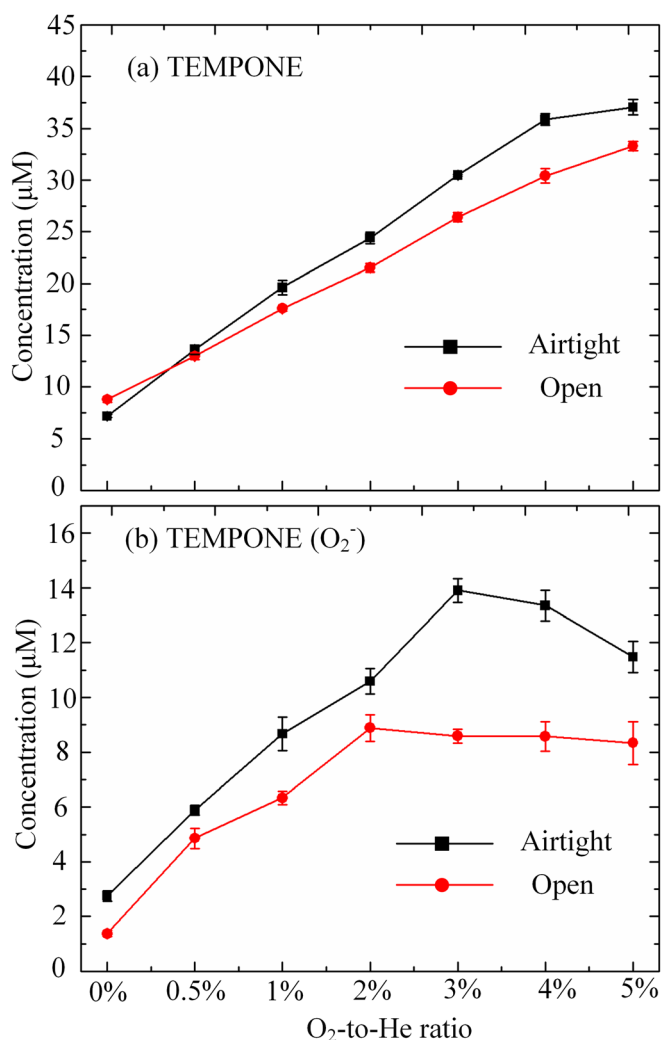


FIG. 6. Concentration of TEMPONE (a) and TEMPONE(O₂⁻) (b) in the liquid phase after 3 min plasma treatment as a function of the O₂ content for the two plasma jets.

the airtight chamber, the concentration of O₂⁻ increases from 2.7 μM to 13.9 μM with the increase in the O₂ fraction from 0% to 3%, and then the concentration decreases to 11.4 μM when 4% O₂ is added to the helium gas. But in the open air condition, the highest concentration of O₂⁻ is 7.9 μM in He + 2% O₂, and the concentration dropped slightly to 7.3 μM in He + 5% O₂. The most important is that the changing trend of the concentration of O₂⁻ is almost the same with the trend of the bactericidal effect with increasing additive O₂ for the two plasma jets, which proves that O₂⁻ and its direct conjugate (HOO) [Eq. (4)] may play an important role for the sterilization



The acid dissociation constant (pKa) of this equation is 4.8,^{44,50} which means that a large number of O₂⁻ will be converted to HOO when the pH of the solution is lower than 4.8. In our experiments, the pH values are always less than 4 with the increase in the additive O₂ after 3 min plasma treatment of the two plasma jets, which can promote the production of the HOO.

Based on previous studies,^{29,51–53} the main production pathways of the aqueous O₂⁻ are the electron attachment by the dissolved oxygen



and the deprotonation of the HOO, which can be produced, for example, by the reaction of ozone with the hydroxyl radical shown in the following equation:



So, the higher concentration of the aqueous O₂⁻ in the airtight chamber condition may be attributed to more electrons reacting with O₂, as well as more ozone dissolved in water. A small amount of O₂ added to the He gas can promote the production of aqueous O₂⁻, but the concentration of aqueous O₂⁻ decreases after the addition of more O₂.

With the use of SOD as an O₂⁻ quencher, the concentration of TEMPONE represents the total concentrations of aqueous ONOO⁻/ONOOH and NO₂. Comparing the experimental data, it can be found that the total concentrations of the both reactive species in the open air condition are higher than that in the airtight chamber condition. According to some reports, the aqueous peroxynitrite is mainly produced by the solvation of gaseous ONOOH and some aqueous reactions in water^{36,54}



In addition, the aqueous NO₂ is also mainly derived from the solvation of gas-phase reactive species and the decomposition of ONOO⁻/ONOOH in the liquid phase. The gaseous ONOOH and NO₂ are produced when the plasma plume meets N₂ or other nitrogen-containing molecules in surrounding air outside the jet nozzle and so does the gaseous NO. The solvation of gaseous NO is then attributed for the production of aqueous ONOOH in water via Eq. (7). Therefore, the concentrations of the two species induced by the plasma jet in the airtight chamber are lower than that in open air in the same discharge power, for the air is excluded and isolated by the quartz cover.

C. Verification experiment

For verifying that O₂⁻ and its direct conjugate (HOO) are playing an essential role for the sterilization, two control experiments are done to regulate the concentrations of O₂⁻ in the solution. The first one is a bactericidal control experiment with SOD as an O₂⁻ quencher and BSA as a control of SOD. Figure 7 shows only the photographs of bactericidal effect in He + 1% O₂ and He + 3% O₂ for the open air condition and the airtight chamber condition, respectively. The results show that there is completely no bactericidal effect after adding SOD in the bactericidal assay with or without the additive O₂ for the two plasma jets. But the bactericidal effect is unaffected by the addition of BSA instead of SOD. Thus, the experimental results can strongly prove that O₂⁻ or

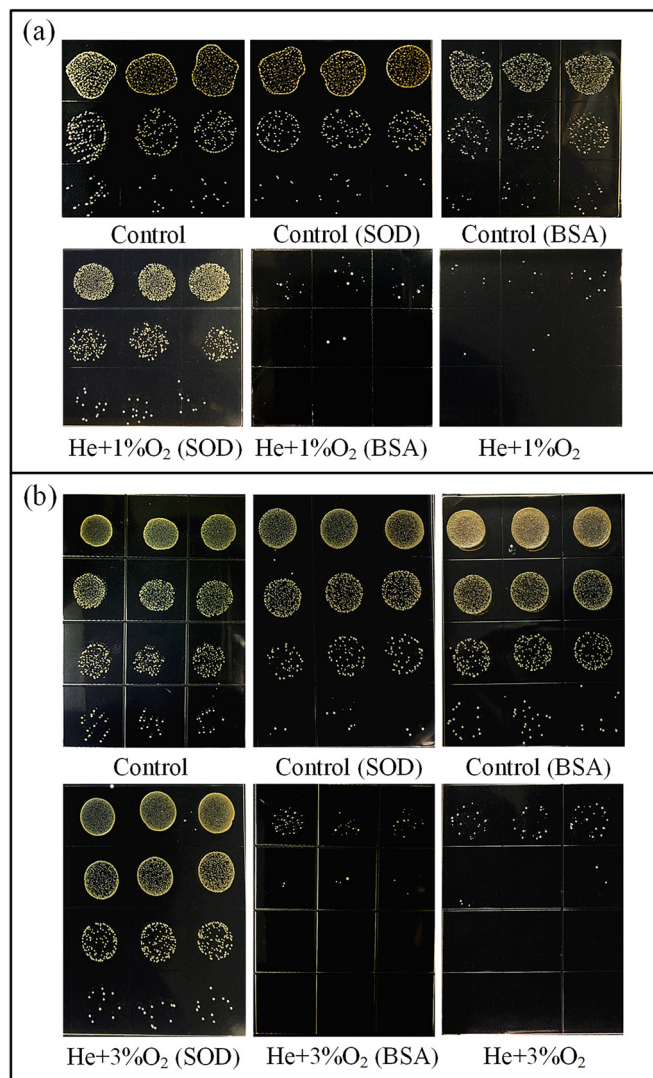


FIG. 7. Photographs of bacterial samples on agar plates with SOD or BSA after treated by the two plasma jets in (a) the open air condition and (b) the airtight chamber condition.

its direct conjugate (HOO) does play a key role for the sterilization and explain the phenomenon that the sterilizing effect in the airtight chamber condition is stronger than that in the open air condition.

To evaluate whether the aqueous O_2^- works along or synergy with other reactive species, the second set of experiments is to use the DW with different dissolved gases to alter the sterilization environment. The DW is bubbled with N_2 or O_2 for 30 min to replace the dissolved gas, and no dissolved air remained in DW after bubbling. Then, the DW in which the dissolved gas consisted of O_2 , N_2 , or air is exposed to a He + 3% O_2 plasma jet for 3 min treatment in the same discharge power. The concentrations of aqueous reactive species and results of sterilization are shown in Fig. 8. It can be seen that the concentrations of H_2O_2 , O_2^- , and DMPO-OH increase when the DW is full of dissolved O_2 . The concentrations of H_2O_2 and O_2^- for the DW with dissolved O_2 almost double that of the DW with dissolved air, which proves that the concentrations of ROS can be significantly

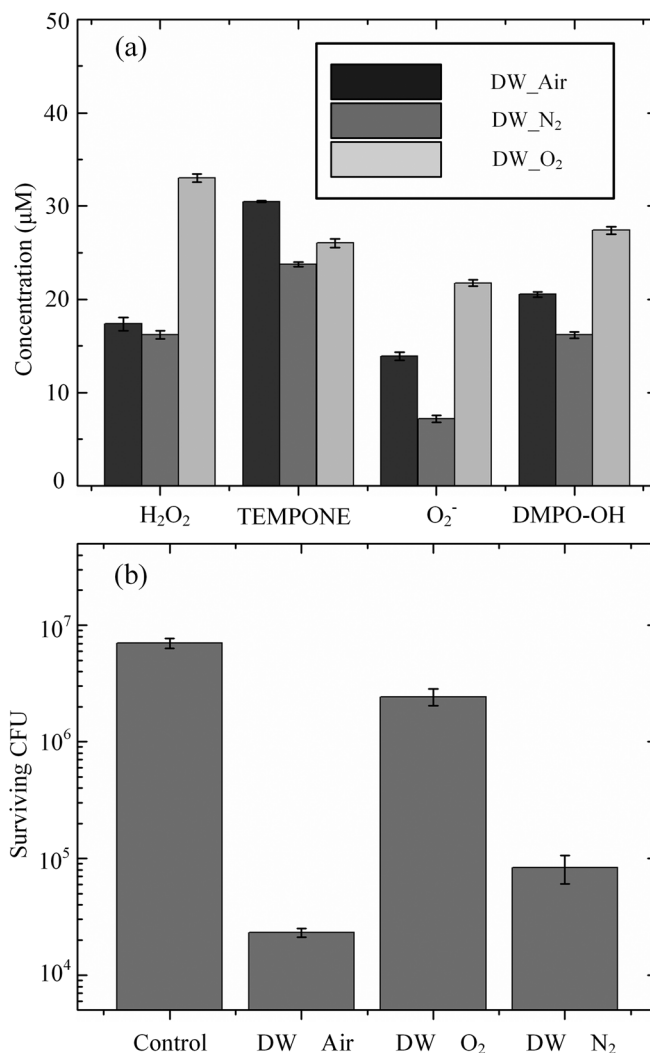


FIG. 8. (a) The concentrations of H_2O_2 , TEMPONE, O_2^- , and DMPO-OH in DW with three different dissolved gases after 3 min He + 3% O_2 plasma treatment in the airtight chamber condition. (b) The corresponding number of surviving cells after 3 min plasma treatment in DW with three different dissolved gases. (DW_Air, DW_O₂, and DW_N₂ represent the deionized water with dissolved air, dissolved O_2 , and dissolved N_2 , respectively.)

increased by increasing the dissolved O_2 in water. In addition, the concentration of TEMPONE with SOD greatly decreases for the DW with dissolved O_2 , which proves that the nitrogen molecules in the DW are excluded. Comparing with the DW with dissolved air, the concentrations of TEMPONE, O_2^- , and DMPO-OH decrease when the DW is full of dissolved N_2 . However, the efficiency of bacterial inactivation of the DW with three different dissolved gases is not in accordance with the concentration of the aqueous O_2^- . The best sterilization effect can be achieved for the DW with dissolved air, and the DW with dissolved O_2 has the worst sterilization effect. The phenomenon shows that although O_2^- or its direct conjugate (HOO) plays a vital role for the sterilization, some kind of RNS is also essential. In the bacterial inactivation, the aqueous O_2^- or its direct conjugate (HOO) does not work along but acts synergistically with certain RNS or some kind of aqueous species synthesized by both. There is a report that the bactericidal species

may be the peroxyntic acid, O_2NOOH , which can be produced by HOO and NO_2 ³⁷



But the hypothesis still needs further experiments to verify.

IV. CONCLUSION

The $He + O_2$ plasma jets in open air and in an airtight chamber are comparatively studied, with respect to their production of gaseous/aqueous reactive species and their antibacterial effects. With the same discharge power, it is found that the discharge intensities and the brightness of the plasma plumes are obviously weaker with an increased content of the additive O_2 for the two plasma jets. In addition, the densities of reactive species in both the plasma jets also decrease monotonically with the increase in the O_2 concentration, except for $O(3p^5P)$ when a small amount of O_2 is added. Penning ionization will lower the discharge voltage with the addition of a small amount of O_2 , but higher voltage is needed after the addition of more O_2 because of gas electronegativity. Besides, the phenomenon of Penning ionization can also explain that the discharge voltage of the plasma jet in open air is lower than that in the airtight chamber.

The bactericidal effects induced by the $He + O_2$ plasma jets in the airtight chamber condition are much greater than that in the open air condition. Regarding the reactive species in the water activated by both the plasma jets, the concentrations of OH and H_2O_2 decrease monotonically, while the concentrations of O_2^- first increase and then decrease. In comparison, the plasma jet in open air has higher densities of gaseous reactive species and a higher concentration of aqueous H_2O_2 but lower concentrations of aqueous OH and O_2^- . The concentration trends of O_2^- for both the plasma jets are similar to their antibacterial effects, and little antibacterial effect is achieved when a scavenger of O_2^- (SOD) is used, indicating that O_2^- should be a main antibacterial agent. Moreover, the verification experiment indicates that it should not be O_2^- alone to achieve the antibacterial effect, and some RNS such as $ONOO^-$ and O_2NOO^- might also play an important role.

ACKNOWLEDGMENTS

This work was supported by the National Science Foundation of China (Grant Nos. 51722705, 51521065, and 51707150), the China Postdoctoral Science Foundation (Grant No. 2017M613134), and the Shaanxi Province Postdoctoral Science Foundation (2017BSHYDZZ11).

¹G. C. Kim, G. J. Kim, S. R. Park, S. M. Jeon, H. J. Seo, F. Iza, and J. K. Lee, *J. Phys. D: Appl. Phys.* **42**, 032005 (2009).

²H. J. Lee, C. H. Shon, Y. S. Kim, S. Kim, G. C. Kim, and M. G. Kong, *New J. Phys.* **11**, 115026 (2009).

³M. Laroussi, *IEEE Trans. Plasma Sci.* **37**, 714 (2009).

⁴M. G. Kong, G. Kroesen, G. Morfill, T. Nosenko, T. Shimizu, J. Van Dijk, and J. L. Zimmermann, *New J. Phys.* **11**, 115012 (2009).

⁵N. Y. Babaeva and M. J. Kushne, *J. Phys. D: Appl. Phys.* **46**, 025401 (2013).

⁶E. Karakas, A. Munyanyi, L. Greene, and M. Laroussi, *Appl. Phys. Lett.* **97**, 143702 (2010).

⁷E. Takai, G. Ohashi, T. Yoshida, K. M. Sorgjerd, T. Zako, M. Maeda, K. Kitano, and K. Shiraki, *Appl. Phys. Lett.* **104**, 023701 (2014).

⁸G. Y. Park, S. J. Park, M. Y. Choi, I. G. Koo, J. H. Byun, J. W. Hong, J. Y. Sim, G. J. Collins, and J. K. Lee, *Plasma Sources Sci. Technol.* **21**, 043001 (2012).

⁹H. Yamazaki, T. Ohshima, Y. Tsubota, H. Yamaguchi, J. A. Jayawardena, and Y. Nishimura, *Dent. Mater. J.* **30**, 384–391 (2011).

¹⁰U. Emi, O. Tomoko, Y. Hiromitsu, I. Satoshi, K. Katsuhisa, M. Nobuko, and M. Yasuko, *Jpn. J. Conserv. Dent.* **58**, 101–108 (2015).

¹¹T. Sato, O. Furuya, K. Ikeda, and T. Nakatani, *Plasma Process. Polym.* **5**, 606–614 (2008).

¹²N. Hayashi, W. Guan, S. Tsutsui, T. Tomari, and Y. Hanada, *Jpn. J. Appl. Phys., Part 1* **45**, 8358–8363 (2006).

¹³H. Q. Feng, R. X. Wang, P. Sun, H. Y. Wu, Q. Liu, J. Fang, W. D. Zhu, F. T. Li, and J. Zhang, *Appl. Phys. Lett.* **97**, 131501 (2010).

¹⁴X. P. Lu, T. Ye, Y. G. Cao, Z. Y. Sun, Q. Xiong, Z. Y. Tang, Z. L. Xiong, J. Hu, Z. H. Jiang, and Y. Pan, *J. Appl. Phys.* **104**, 053309 (2008).

¹⁵R. Bussiahn, R. Brandenburg, T. Gerling, E. Kindel, H. Lange, N. Lembke, K. D. Weltmann, T. von Woedtke, and T. Kocher, *Appl. Phys. Lett.* **96**, 143701 (2010).

¹⁶J. F. Kolb, A. A. H. Mohamed, R. O. Price, R. J. Swanson, A. Bowman, R. L. Chiavarini, M. Stacey, and K. H. Schoenbach, *Appl. Phys. Lett.* **92**, 241501 (2008).

¹⁷X. Lu, G. V. Naidis, M. Laroussi, S. Reuter, D. B. Graves, and K. Ostrikov, *Phys. Rep.* **630**, 1–84 (2016).

¹⁸E. Takai, S. Ikawa, K. Kitano, J. Kuwabara, and K. Shirki, *J. Phys. D: Appl. Phys.* **46**, 295402 (2013).

¹⁹X. T. Deng, J. J. Shi, and M. G. Kong, *J. Appl. Phys.* **101**, 074701 (2007).

²⁰H. Xu, D. X. Liu, W. J. Xia, C. Chen, W. T. Wang, Z. J. Liu, X. H. Wang, and M. G. Kong, *Phys. Plasmas*, **25**, 013520 (2018).

²¹D. B. Graves, *J. Phys. D: Appl. Phys.* **45**, 263001 (2012).

²²H. Xu, C. Chen, D. X. Liu, D. H. Xu, Z. J. Liu, X. H. Wang, and M. G. Kong, *J. Phys. D: Appl. Phys.* **50**, 245201 (2017).

²³X. P. Lu, Z. H. Jiang, Q. Xiong, Z. Y. Tang, X. W. Hu, and Y. Pan, *Appl. Phys. Lett.* **92**, 081502 (2008).

²⁴N. Bai, P. Sun, H. X. Zhou, H. Y. Wu, R. X. Wang, F. X. Liu, W. D. Zhu, J. L. Lopez, J. Zhang, and J. Fang, *Plasma Process. Polym.* **8**, 424–431 (2011).

²⁵Y. Sun, S. Yu, P. Sun, H. Y. Wu, W. D. Zhu, W. Liu, J. Zhang, J. Fang, and R. Y. Li, *PLoS One* **7**, e40629 (2012).

²⁶H. M. Joh, J. Y. Cho, S. J. Kim, T. H. Chung, and T. H. Kang, *Sci. Rep.* **4**, 6638 (2014).

²⁷X. P. Lu and K. Ostrikov, *Appl. Phys. Rev.* **5**, 031102 (2018).

²⁸J. Y. Kim, D. H. Lee, J. Ballato, W. Cao, and S. O. Kim, *Appl. Phys. Lett.* **101**, 224101 (2012).

²⁹X. H. Zhang, M. J. Li, R. L. Zhou, K. C. Feng, and S. Z. Yang, *Appl. Phys. Lett.* **93**, 21502 (2008).

³⁰H. M. Joh, S. J. Kim, T. H. Chung, and S. H. Leem, *Appl. Phys. Lett.* **101**, 053703 (2012).

³¹A. Tani, Y. Ono, S. Fukui, S. Ikawa, and K. Kitano, *Appl. Phys. Lett.* **100**, 254103 (2012).

³²Y. Gorbanev, D. O. Connell, and V. Chechik, *Chem. Eur. J.* **22**, 3496–3505 (2016).

³³C. E. Anderson, N. R. Cha, A. D. Lindsay, D. S. Clark, and D. B. Graves, *Plasma Chem. Plasma Process.* **36**, 1393 (2016).

³⁴H. Tresp, M. U. Hammer, and K.-D. Weltmann Reuter, *J. Phys. D: Appl. Phys.* **46**, 435401 (2013).

³⁵S. Dikalov, M. Skatchkov, and E. Bassenge, *Biochem. Biophys. Res. Commun.* **230**, 54–57 (1997).

³⁶C. Chen, F. Y. Li, H. L. Chen, and M. G. Kong, *J. Phys. D: Appl. Phys.* **50**, 445208 (2017).

³⁷S. Ikawa, A. Tani, Y. Nakashima, and K. Kitano, *J. Phys. D: Appl. Phys.* **49**, 425401 (2016).

³⁸R. L. Baehner, S. K. Murrmann, J. Davis, and R. B. Johnston, Jr., *J. Clin. Invest.* **56**, 571 (1975).

³⁹R. B. Johnston, Jr., B. B. Keele, Jr., H. P. Misra, J. E. Lehmyer, L. S. Webb, R. L. Baehner, and K. V. Rajagopalan, *J. Clin. Invest.* **55**, 1357 (1975).

⁴⁰Y. Yang, W. C. Wang, D. Z. Yang, L. Jia, and S. Zhang, *J. Electrostat.* **70**, 356 (2012).

⁴¹R. E. Walkup, K. L. Saenger, and G. S. Selwyn, *J. Chem. Phys.* **84**, 2668 (1986).

- ⁴²Q. Zhang, Y. Liang, H. Feng, R. Ma, Y. Tian, J. Zhang, and J. Fang, *Appl. Phys. Lett.* **102**, 203701 (2013).
- ⁴³M. J. Traylor, M. J. Pavlovich, S. Karim, P. Hait, Y. Sakiyama, D. S. Clark, and D. B. Graves, *J. Phys. D: Appl. Phys.* **44**, 472001 (2011).
- ⁴⁴S. Ikawa, K. Kitano, and S. Hamaguchi, *Plasma Process. Polym.* **7**, 33–42 (2010).
- ⁴⁵S. S. Korshunov and J. A. Imlay, *Mol. Microbiol.* **43**, 95–106 (2002).
- ⁴⁶F. X. Liu, P. Sun, N. Bai, Y. Tian, H. X. Zhou, S. C. Wei, Y. H. Zhou, J. Zhang, W. D. Zhu, K. Becker, and J. Fang, *Plasma Process. Polym.* **7**, 231–236 (2010).
- ⁴⁷U. K. Ercan, J. Smith, H. F. Ji, A. D. Brooks, and S. G. Joshi, *Sci. Rep.* **6**, 20365 (2016).
- ⁴⁸Z. Y. Chen, D. X. Liu, C. Chen, D. H. Xu, Z. J. Liu, W. J. Xia, M. Z. Rong, and M. G. Kong, *J. Phys. D: Appl. Phys.* **51**, 325201 (2018).
- ⁴⁹P. Bruggeman and D. C. Schram, *Plasma Sources Sci. Technol.* **19**, 045025 (2010).
- ⁵⁰R. B. Zhang, L. M. Wang, Y. Wu, Z. C. Guan, and Z. D. Jia, *IEEE Trans. Plasma Sci.* **34**, 1370 (2006).
- ⁵¹C. Chen, D. X. Liu, Z. C. Liu, A. J. Yang, H. L. Chen, G. Shama, and M. G. Kong, *Plasma Chem. Plasma Process.* **34**, 403 (2014).
- ⁵²C. A. J. van Gils, S. Hofmann, B. K. H. L. Boekema, R. Brandenburg, and P. J. Bruggeman, *J. Phys. D: Appl. Phys.* **46**, 175203 (2013).
- ⁵³D. X. Liu, P. Bruggeman, F. Iza, M. Z. Rong, and M. G. Kong, *Plasma Sources Sci. Technol.* **19**, 025018 (2010).
- ⁵⁴W. Tian and M. J. Kushner, *J. Phys. D: Appl. Phys.* **47**, 165201 (2014).